Theory and three-dimensional numerical simulation of sound propagation along a long enclosure with side opening

S. H. K. CHU[1]; S. K. TANG[2]

[1, 2] Department of Building Services Engineering, The Hong Kong Polytechnic University, Hong Kong, China

ABSTRACT

The sound properties along a long rectangular enclosure with a circular source on the top wall and rectangular opening at the side wall are studied. A mathematical model of average pressure at an opening contributed by the sound source and assuming air piston at the opening is derived in terms of the acoustic mode for a rigid duct. Three-dimensional numerical modelling is conducted to compare the theoretical prediction. The computational domain of interest is a long rectangular block associated with an opening connected to a free field environment. Non-reflecting portion is applied to each end of the domain. Sound pressure variations of discrete propagating mode are investigated. Interactions between the resonance of closed duct and effect of the opening are demonstrated at various frequencies. Comparisons indicate that the theoretical predictions give consistent results with that of numerical models. Precision of the radiation impedance of aperture is found crucial to the accuracy of mathematical model. This study approach including the theory and simulation provides a constructive framework for further examination of related subjects.

Keywords: Sound propagation, Long enclosure, Side opening
I-INCE Classification of Subjects Number(s): 23

1. INTRODUCTION

Long rectangular enclosures including air ducts, tunnels and the long tunnel like corridors are common features in building elements and infrastructural. Noise propagation and reverberation in such long closed enclosures have been studied in the past few decades (1, 2). Rectangular opening is found popular in this kind of long enclosure. Noise propagation along a long rectangular enclosure with a rectangular opening at the side wall is interested in this study.

The present study approach is to derive a mathematical model to compare the in-duct sound behavior of three-dimensional numerical model. Contribution of a circular sound source on the top wall is adopted (3). Special efforts are made in examining how the opening size affecting the results.

2. THEORETICAL PREDICTION

2.1 Average acoustic pressure at the opening

As illustrated in Figure 1, a rectangular air piston of size w x h is flush-mounted on the side wall of the duct with interior of height a and width b. A circular sound source is fixed on the top wall of the rectangular duct. The case for consideration is the sound field of excitation of acoustic modes by the sound source with a side opening in a straight, hard-walled duct of constant area of cross section and infinite length.

The fluid loading in term of average pressure acting on a single air piston at the opening can be set as follows (4, 5).

[1] 09902976r@connect.polyu.hk
[2] shiu-keung.tang@polyu.edu.hk

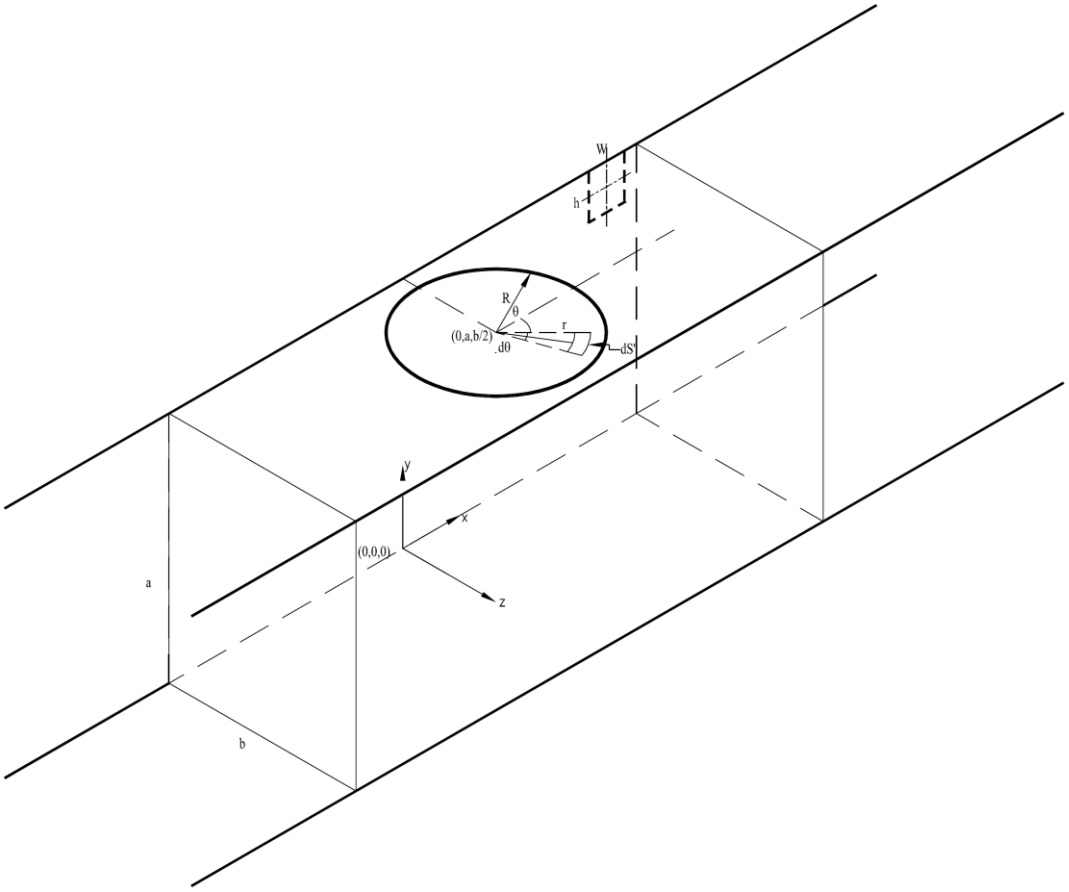

Figure 1 – Geometry of the rectangular side wall opening and flush-mounted circular sound source

The average acoustic pressure at the opening contributed by the circular source is:

$$\frac{1}{hw}\iint_{s} p_s(x,y)dS \tag{1}$$

where $dS=dxdy$ and p_s is pressure wave generated by the source
The self-contribution of the air piston at the opening:

$$\frac{1}{hw}\iint_{s} VF(x,y)dS \tag{2}$$

$$\frac{1}{hw}\int_{x_1-w/2}^{x_1+w/2}\int_{a-h}^{a} p_s(x,y|x_1,a-h/2)dxdy+\frac{1}{hw}\int_{-w/2}^{+w/2}\int_{a-h}^{a} VF(x,y)dxdy=VZ_r \tag{3}$$

V is the velocity to be solved and Z_r is the radiation impedance of the air piston. Following clauses elaborate the above mathematical model in details.

2.2 General solution for the wave propagation of a wall-mounted air piston

The general solution for the wave propagation of a flush-mounted air piston in a hard-walled duct of constant cross section and infinite length is (4):

$$p(x,y,z,t) = \frac{\rho_o}{2ab}\sum_{m,n} c_{mn}\psi_{mn}(y,z)\oint \psi^*_{mn}(y',z')V(x',y',z',t)\left[H(x-x')e^{\frac{-i\omega(x-x')}{c_{mn}}}+H(x'-x)e^{\frac{i\omega(x-x')}{c_{mn}}}\right]dS' \tag{4}$$

where

$$\psi_{mn}(y,z) = \sqrt{(2-\delta_{0m})(2-\delta_{0n})}\cos\left(\frac{m\pi y}{a}\right)\cos\left(\frac{n\pi z}{b}\right)$$

$$\left(\frac{c}{c_{mn}}\right)^2 = 1-\left(\frac{\omega_{mn}}{\omega}\right)^2, \qquad \left(\frac{\omega_{mn}}{c}\right)^2 = \left(\frac{m\pi}{a}\right)^2+\left(\frac{n\pi}{b}\right)^2$$

and V is a constant. Since the rectangular air piston is mounted on the top side wall,

$$z' = 0, \text{ center of } x' = 0 \text{ and } y' = a-\frac{h}{2}$$

The integral is:

$$\sqrt{(2-\delta_{0m})(2-\delta_{0n})}\oint \cos\frac{m\pi y'}{a}\cos\frac{n\pi z'}{b}\left[H(x-x')e^{-i\beta_{mn}(x-x')}+H(x'-x)e^{i\beta_{mn}(x-x')}\right]dS' \tag{5}$$

where

$$dS' = dx'dy'$$

$$\beta_{mn} = \frac{\omega}{c_{mn}} = \sqrt{\left(\frac{\omega}{c}\right)^2-\left(\frac{m\pi}{a}\right)^2-\left(\frac{n\pi}{b}\right)^2}$$

$$\cos\frac{n\pi z'}{b} = 1$$

$$\int_{a-h}^{a}\cos\frac{m\pi y'}{a}dy' = \begin{cases} h & ,m=0 \\ (-1)^m h\sin\left(\frac{m\pi h}{a}\right)/\left(\frac{m\pi h}{a}\right) & ,m\neq 0 \end{cases}$$

2.3 Self-contribution of air piston

The self-contribution of the side aperture is derived as below.

$$|x| \le +w/2$$

$$\int_{-w/2}^{x} e^{-i\beta_{mn}(x-x')}dx' + \int_{x}^{+w/2} e^{i\beta_{mn}(x-x')}dx' = \frac{2}{i\beta_{mn}}\left[1-e^{-i\beta_{mn}w/2}\cos(\beta_{mn}x)\right] \tag{6}$$

The whole integral is, for m = 0:

$$\sqrt{(2-\delta_{0m})(2-\delta_{0n})}\ \frac{2h}{i\beta_{mn}}\left[1-e^{-i\beta_{mn}w/2}\cos(\beta_{mn}x)\right]$$

for $m \neq 0$,

$$(-1)^m\sqrt{(2-\delta_{0m})(2-\delta_{0n})}\ \frac{2h}{i\beta_{mn}}\left[1-e^{-i\beta_{mn}w/2}\cos(\beta_{mn}x)\right]\frac{\sin\left(\frac{m\pi h}{a}\right)}{\left(\frac{m\pi h}{a}\right)}$$

The solution, for m = 0:

$$p(x,y,z,t) = \omega h\frac{\rho_o V e^{-i\omega t}}{ab}\sum_{m,n}\sqrt{(2-\delta_{0m})(2-\delta_{0n})}\frac{1-e^{-i(\frac{w}{2})\sqrt{k^2-k_{mn}^2}}\cos(x\sqrt{k^2-k_{mn}^2})}{i(k^2-k_{mn}^2)}\psi_{mn}(y,z) \tag{7}$$

for $m \neq 0$,

$$p(x,y,z,t) = \omega h\frac{\rho_o V e^{-i\omega t}}{ab} \times\sum_{m,n}\sqrt{(2-\delta_{0m})(2-\delta_{0n})}(-1)^m\frac{\sin\left(\frac{m\pi h}{a}\right)\left[1-e^{-i(\frac{w}{2})\sqrt{k^2-k_{mn}^2}}\cos(x\sqrt{k^2-k_{mn}^2})\right]}{i\left(\frac{m\pi h}{a}\right)(k^2-k_{mn}^2)}\psi_{mn}(y,z) \tag{8}$$

Therefore, the average pressure of the single air piston:

$$\bar{p} = \frac{V}{hw}\int_{-w/2}^{+w/2}\int_{a-h}^{a}F(x,y)dxdy \tag{9}$$

$$\int_{-w/2}^{+w/2} \cos(x\sqrt{k^2-k_{mn}^2})\,dx = \frac{2}{\sqrt{k^2-k_{mn}^2}}\sin\left(\frac{w}{2}\sqrt{k^2-k_{mn}^2}\right)$$

$$\int_{a-h}^{a} \cos\frac{m\pi y}{a}\,dy = \begin{cases} h & ,m=0 \\ (-1)^m h \sin\left(\frac{m\pi h}{a}\right)/\left(\frac{m\pi h}{a}\right) & ,m\neq 0 \end{cases}$$

One can note that, for m = 0:

$$\bar{p}(x_1, a-d/2, 0) = V\frac{\omega h\rho_o}{wab}\sum_{m,n}\frac{(2-\delta_{0m})(2-\delta_{0n})\left[w-\frac{2e^{-i(\frac{w}{2})\sqrt{k^2-k_{mn}^2}}}{\sqrt{k^2-k_{mn}^2}}\sin\left(\frac{w}{2}\sqrt{k^2-k_{mn}^2}\right)\right]}{i(k^2-k_{mn}^2)} \quad (10)$$

for $m \neq 0$,

$$\bar{p}(x_1, a-h/2, 0) = V\frac{\omega h\rho_o}{wab}\sum_{m,n}\frac{(2-\delta_{0m})(2-\delta_{0n})\sin^2\left(\frac{m\pi h}{a}\right)\left[w-\frac{2e^{-i(\frac{w}{2})\sqrt{k^2-k_{mn}^2}}}{\sqrt{k^2-k_{mn}^2}}\sin\left(\frac{w}{2}\sqrt{k^2-k_{mn}^2}\right)\right]}{i\left(\frac{m\pi h}{a}\right)^2(k^2-k_{mn}^2)} \quad (11)$$

2.4 Acoustic pressure at the opening contributed by the source

This section describes the wave field by a circular sound source. A mathematical model of the pressure wave generated by assuming a flush-mounted circular piston vibration as the sound source for rigid duct has been derived (3), for even n:

$$p_s(x,y,z,t) = \pi\omega R\frac{\rho_o V_s e^{-i\omega t}}{ab}\sum_{m,n}\sqrt{(2-\delta_{0m})(2-\delta_{0n})}(-1)^{m+\frac{n}{2}}\frac{J_1\left(R\sqrt{k^2-k_{m0}^2}\right)}{\sqrt{k^2-k_{mn}^2}\sqrt{k^2-k_{m0}^2}}\psi_{mn}(y,z)e^{-i|x|\sqrt{k^2-k_{mn}^2}} \quad (12)$$

The average pressure of source contribution to the side opening is as below.

$$\bar{p_s} = \frac{1}{hw}\int_{x_1-w/2}^{x_1+w/2}\int_{a-h}^{a} p_s(x,y|x_1,a-h/2)dxdy \quad (13)$$

$$\int_{x_1-w/2}^{x_1+w/2} e^{-i|x|\sqrt{k^2-k_{mn}^2}}dx = \frac{2\sin\left(\frac{w}{2}\sqrt{k^2-k_{mn}^2}\right)}{\sqrt{k^2-k_{mn}^2}}e^{-i|x_1|\sqrt{k^2-k_{mn}^2}}$$

$$\int_{a-h}^{a} \cos\frac{m\pi y}{a}\,dy = \begin{cases} h & ,m=0 \\ (-1)^m h \sin\left(\frac{m\pi h}{a}\right)/\left(\frac{m\pi h}{a}\right) & ,m\neq 0 \end{cases}$$

One can note that, for m = 0:

$$\bar{p_s}(x_1, a-h/2, 0) = 2\pi\omega R\frac{\rho_o V_s}{abw}\sum_{m,n}(-1)^{\frac{n}{2}}\frac{(2-\delta_{0m})(2-\delta_{0n})J_1\left(R\sqrt{k^2-k_{m0}^2}\right)}{(k^2-k_{mn}^2)\sqrt{k^2-k_{m0}^2}}\sin\left(\frac{w}{2}\sqrt{k^2-k_{mn}^2}\right)e^{-i|x_1|\sqrt{k^2-k_{mn}^2}} \quad (14)$$

for $m \neq 0$,

$$\bar{p_s}(x_1, a-h/2, 0) = 2\pi\omega R\frac{\rho_o V_s}{abw} \times \sum_{m,n}(-1)^{2m+\frac{n}{2}}\frac{(2-\delta_{0m})(2-\delta_{0n})\sin\left(\frac{m\pi h}{a}\right)J_1\left(R\sqrt{k^2-k_{m0}^2}\right)}{\left(\frac{m\pi h}{a}\right)(k^2-k_{mn}^2)\sqrt{k^2-k_{m0}^2}}\sin\left(\frac{w}{2}\sqrt{k^2-k_{mn}^2}\right)e^{-i|x_1|\sqrt{k^2-k_{mn}^2}} \quad (15)$$

2.5 Radiation impedance of a rectangular air piston

A flat rectangular piston mounted flush within an infinite baffle is assumed in the present study. The radiation impedance is as below but the width to height ratio (w/h) is neither very large nor very small (1).

$$Z = \frac{w^2\theta(kw) - h^2\theta(kh) - iw^2\varphi(kw) + ih^2\varphi(kh)}{w^2 - h^2} \tag{16}$$

where

$$\theta(x) = 1 - \frac{4[1 - J_0(x)]}{x^2}$$

$$\varphi(x) = \frac{8}{\pi x}[1 - \frac{\pi}{2x}H_0(x)]$$

$J_0(x)$ is Bessel function of zero order; $H_0(x)$ is Struve function of zero order.

In consideration of the duct thickness of aperture δ, the incident and reflected waves are as below (6).

$$P_i = Ie^{-ikz},\ P_r = Re^{ikz}$$

At z= 0,

Continuity of pressure: $I+R=P_0$

Continuity of volume velocity: $U_i+U_r=U_0$

$$\frac{I - R}{z_g} = \frac{P_0}{z_0}$$

$z_g=\rho c/S$ where S is the cross-section area of aperture.

$$Z = \frac{z_0}{z_g} = \frac{I + R}{I - R}$$

$$\frac{R}{I} = \frac{Z - 1}{Z + 1}$$

At z= δ,

Continuity of pressure: $P_i+P_r=P_\delta$

Continuity of volume velocity: $U_i+U_r=U_\delta$

$$\frac{Ie^{-ik\delta} - Re^{ik\delta}}{z_g} = \frac{P_\delta}{z_r}$$

$$\frac{e^{-ik\delta} - (\frac{R}{I})e^{ik\delta}}{z_g} = \frac{e^{-ik\delta} + (\frac{R}{I})e^{ik\delta}}{z_r}$$

The radiation impedance with the effect of aperture thickness is:

$$Z_r = \frac{z_r}{z_g} = \frac{e^{-ik\delta} + (\frac{R}{I})e^{ik\delta}}{e^{-ik\delta} - (\frac{R}{I})e^{ik\delta}} = \frac{Z - itan(k\delta)}{1 - iZtan(k\delta)} \tag{17}$$

3. FINITE ELEMENT COMPUTATIONAL MODEL

The numerical model is established in following principle (7). The Helmholtz equation, which describes harmonic wave propagation in medium without damping, is represented as below.

$$\nabla^2 p + k^2 p = 0 \tag{18}$$

where p and k denote the acoustic pressure and the wave number.

The boundary condition associated with all surfaces of the duct follows that of a rigid wall of vanishing normal acoustic particle velocity.

$$\left.\frac{\partial p}{\partial n}\right|_{\text{wall}} = 0 \tag{19}$$

where n represents the outward normal direction of a boundary.

The interactions between sound in the air and the three-dimensional solid duct with an opening are modelled by using the finite element software COMSOL Multiphysics. The inhomogeneous wave equation as below is implemented in the numerical model (8, 9).

$$\nabla \cdot (\frac{1}{\rho_0}(\nabla p - q)) - \frac{\omega^2 p}{\rho_0 c^2} = Q \tag{20}$$

where the dipole source q and monopole source Q are set to be zero, ρ_0 is the fluid density, c is the speed of sound. Eq.18 is simply formed as $\omega/c=k$.

The boundary conditions of wall, sound source and the free field environment are introduced. The sound-hard boundary is

$$\mathrm{n} \cdot (\frac{1}{\rho_0} (\nabla p - q)) = 0 \quad (21)$$

This turns out to be Eq.19 for zero dipole source. The circular sound source is set to be the normal acceleration boundary condition. A unity inward acceleration enters at the circular boundary.

The opening is connected to the free field environment. An absorbing perfectly matched layer (PML) in cylindrical type is added. It applies approximate the boundary at infinity in an exterior problem and allows an outgoing wave to leave the computational domain with no or minimal reflections (9). PML is also attached to each duct end in order to eliminate the effect of reflections at the ends of computational domain. PMLs absorbing in Cartesian coordinate of *x* direction are set.

4. GEOMETRY DATA AND SETTINGS OF THE SIMULATED MODEL

The acoustic model of interest in the present study is set to be a 0.8-metre long duct of internal uniform cross section area of 0.082m in width and 0.092m in height. The aspect ratio of the cross section is around 1.12 which can reduce the opportunity of modal overlapping occurred. The duct thickness is fixed to 1mm. The sound source is in 0.046m diameter. The centre of the opening is allocated along *x*-axis arbitrarily at 0.162m (x_1=9mm×18). Cases of following sizes of opening are selected for the numerical analysis.

Table 1 – Selected cases for change of opening size

Opening	Height (mm)	Width (mm)
Case 1	9 (approximate *a*/10)	8
Case 2	13.5	12
Case 3	18	16

The diameter of the free field domain is 80mm which is large compared to the dimension of opening (Figure 2). The PML width of the free field is 20mm. PMLs with 0.5m in length at two ends have the same uniform cross section of the acoustic model (Figure 3). Each cases performs numerical analysis for series of frequency in the model.

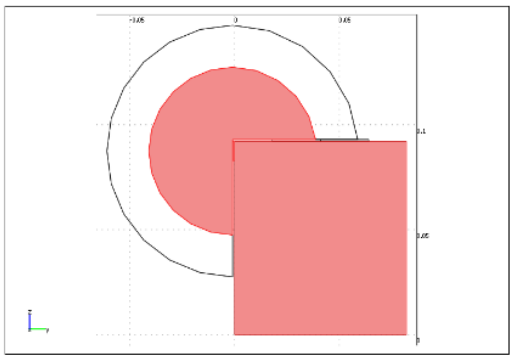

Figure 2 – A section of the computational model

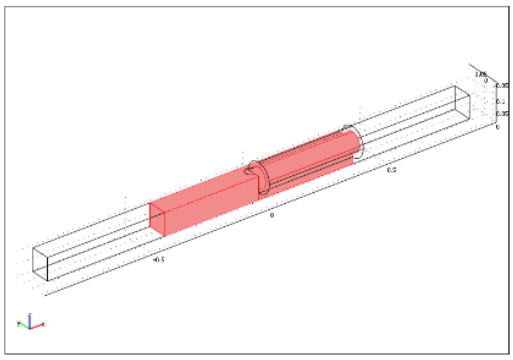

Figure 3 – PML at two ends of the model

5. RESULTS AND DISCUSSIONS

Acoustic mode shape across the cross section of the duct with various frequencies are generated. For instance, pattern at the resonance near the eigen-frequency at mode 01 of numerical model is captured at the centre of opening as shown in Figure 4. The form of cylindrical sound radiation at the opening is noted.

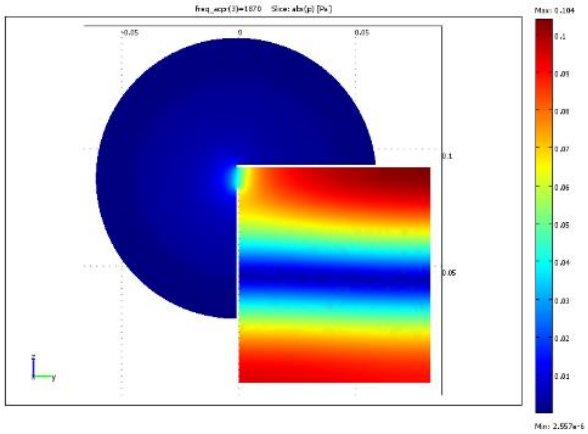

Figure 4 – Pattern at the resonance frequency, mode 01, 9mm height opening

In-duct modal decomposition (10, 11) is adopted to analyse the computational data of sound pressure over the concerned internal cross sections. The interval of cross section along x direction is 9mm and the frequency resolution is 10Hz. Data from 37 sections and 11 frequencies (total 407 points) were collected for each cases. Results obtained are considered as the target values for comparison.

R=0.023, ρ_0=1.25kg/m^3, c=343m/s, a=0.092m and b=0.082m. The source normal acceleration is unity and $\dot{V}_s = -i\omega V_s$, V_s is $i/(kc)$. The acoustic velocity normal direction to the opening V of Eq.3 can be solved by section 2 mathematically. Thus, the predicated sound field along the duct can be calculated by the contribution of the opening Eq.7, 8 and the force from source Eq.12.

The root mean square (RMS) percentage error is applied as the measure of accuracy of a validation which is defined by the formula. Results of various cases are shown in Table 2.

RMS percentage error = $100\%\sqrt{\frac{1}{n}\sum_{t=1}^{n}(\frac{T_t-P_t}{T_t})^2}$

n is number of fitted points

T_t are the target values obtained from 3-D numerical model

P_t are the prediction values calculated by mathematical model

Table 2 – RMS percentage error of data from COMSOL against MATLAB

Case	Opening size (mm)	Frequency range 250-350Hz	Frequency range 1850-1950Hz
1a	9 x 8 (without duct thickness correction)	0.52%	1.22%
1b	9 x 8	0.32%	0.74%
2	13.5 x 12	0.67%	1.52%
3	18 x 16	1.10%	2.50%

Figure 5, 6 illustrate the findings of Case 1a and 1b at frequency range of 250-350Hz (plane mode). Comparisons show that the theoretical predictions provide good agreement with the results from numerical models. The presence of effect of duct thickness at the radiation impedance of aperture gives a better accuracy on the mathematical model.

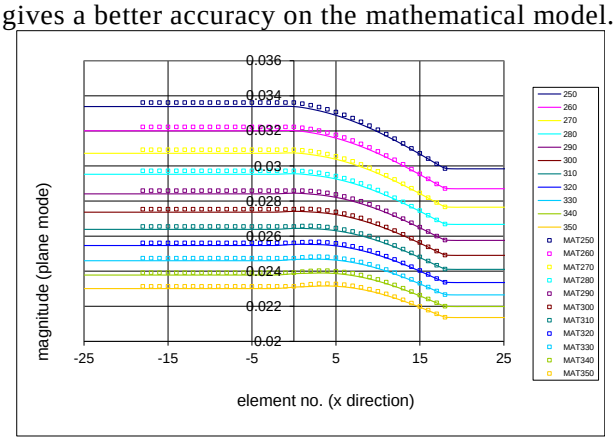

Figure 5 – Case 1a (without duct thickness)

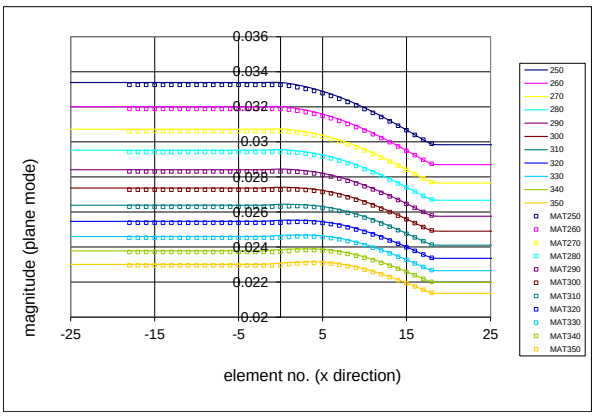

Figure 6 – Case 1b

The error increases as opening size enlarges. Figure 7 illustrates the worst case in the present study which is 2.5% error. Such deviation may be due to the existence of uneven acoustic velocity and sound diffraction at the opening in numerical modelling. It is expected that acoustic velocity of *x*-component could be happened especially in propagating mode.

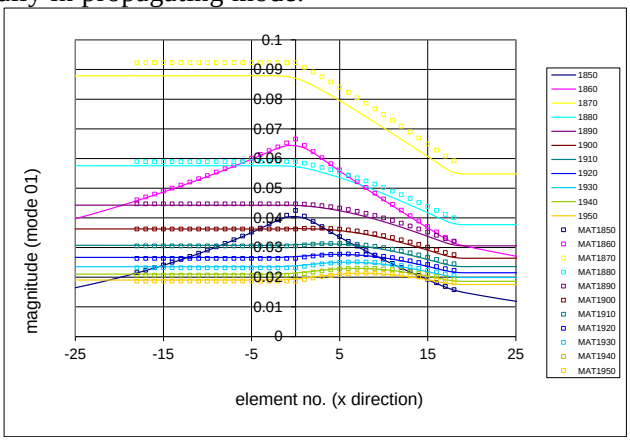

Figure 7 – Case 3 at 1850-1950Hz

6. CONCLUSIONS

The acoustical properties in a long rectangular duct in the presence of a rectangular side wall opening and a circular sound source are reviewed. A mathematical model of interior sound field is derived. Three-dimensional numerical model is also implemented to compare with the predictions by the mathematical model. Values calculated from theoretical prediction give consistent acoustical behaviour with that of numerical model.

Results are convinced that precision of the radiation impedance of aperture is important to the accuracy of theoretical prediction. The present study approach formulate a construction framework for further investigation of related subjects such as understanding of sound propagation along a partial/ discontinuous enclosure.

ACKNOWLEDGEMENTS

S. H. K. Chu is supported by grants from The Hong Kong Polytechnic University and Far East Consulting Engineers Limited.

REFERENCES

1. Morse PM, Ingard KU. Theoretical Acoustics. New York: McGraw Hill; 1968.
2. Doak PE. Excitation, transmission and radiation of sound from source distributions in hard-walled ducts of finite length (I): the effects of duct cross-section geometry and source distribution space-time pattern. J. Sound Vib. 1973; 31: 1–72.
3. Chu SHK, Tang SK. Theoretical prediction and experimental modal analysis of sound propagation along a long enclosure. Proc. ICSV19, Vilnius, Lithuania, July 8-12, 2012.
4. Huang L. A theory of reactive control of low-frequency duct noise. J. Sound Vib. 2000; 238(4): 575-594.
5. Tang SK. Narrow sidebranch arrays for low frequency duct noise control. J. Acoust. Soc. Am. 2012; 132 (5): 3086-3097.
6. Kinsler LE, Frey AR, Coppens AB, Sanders JV. Fundamentals of Acoustics. 4th ed. New York: Wiley; 2000.
7. Chu SHK, Tang SK. Three-dimensional numerical modelling of sound propagation in a long partial enclosure. Proc. Inter-noise 2013; 15-18 September 2013; Innsbruck, Austria 2013.
8. Floody SE, Venegas R, Leighton FC. Optimal design of slit resonators for acoustic normal mode control in rectangular room. Proc. COMSOL Conference; Paris 2010.
9. COMSOL AB. COMSOL Multiphysics Modelling Guide. Ver. 3.5a. 2008.
10. Morse PM, Feshbach H. Methods of Theoretical Physics. Vol. 1. New York: McGraw Hill; 1953.
11. Abom M. Modal decomposition in ducts based on transfer function measurements between microphone pairs. J. Sound Vib. 1989; 135(1): 95-114.